

UV and IR Spectroscopy of Cryogenically Cooled, Lanthanide-Containing Ions in the Gas Phase

**Yoshiya Inokuchi,^{a,*} Masashi Kaneko,^{a,†} Takumi Honda,^a Satoru Nakashima,^a
Takayuki Ebata,^a and Thomas R. Rizzo^b**

*Department of Chemistry, Graduate School of Science, Hiroshima University,
Higashi-Hiroshima, Hiroshima 739-8526, Japan, and Laboratoire de Chimie Physique
Moléculaire, École Polytechnique Fédérale de Lausanne, Lausanne CH-1015,
Switzerland*

E-mail: y-inokuchi@hiroshima-u.ac.jp

Phone: +81(Japan)-82-424-7101

*To whom correspondence should be addressed.

^aHiroshima University

^bÉcole Polytechnique Fédérale de Lausanne

[†]Present address: Nuclear Science and Engineering Directorate, Japan Atomic Energy
Agency, Shirakatashirane 2-4, Tokai-mura, Naka-gun, Ibaraki 319-1195, Japan

Abstract

We measure UV and IR spectra in the gas phase for EuOH^+ , EuCl^+ , and TbO^+ ions, which are produced by an electrospray ionization source and cooled to ~ 10 K in a cold, 22-pole ion trap. The UV photodissociation (UVPD) spectra of these ions show a number of sharp, well-resolved bands in the $30000\text{--}38000\text{ cm}^{-1}$ region, although a definite assignment of the spectra is difficult because of a high degree of congestion. We also measure an IR spectrum of the EuOH^+ ion in the $3500\text{--}3800\text{ cm}^{-1}$ region by IR-UV double resonance spectroscopy, which reveals an OH stretching band at 3732 cm^{-1} . We perform density functional theory (DFT) and time-dependent DFT (TD-DFT) calculations of these ions in order to examine the nature of the transitions. The DFT results indicate that the states of highest spin multiplicity (octet for EuOH^+ and EuCl^+ , and septet for TbO^+) is substantially more stable than other states of lower spin multiplicity. The TD-DFT calculations suggest that the UV absorption of the EuOH^+ and EuCl^+ ions arises from $\text{Eu}(4f) \rightarrow \text{Eu}(5d, 6p)$ transitions, whereas the electronic transitions of the TbO^+ ion are mainly due to the electron promotion of $\text{O}(2p) \rightarrow \text{Tb}(4f, 6s)$. The UVPD results of the lanthanide-containing ions in this study suggest the possibility of using lanthanide ions as “conformation reporters” for the gas-phase spectroscopy for large molecules.

Keywords: lanthanide, ultraviolet spectroscopy, conformation, cold ion trap

1. Introduction

Ultraviolet spectroscopy in the gas phase is a sensitive conformational probe of large molecular systems, such as amino acids and peptides.¹ For example, tyrosine has more than 10 conformers in the gas phase, and they give distinct S_1 – S_0 origin bands within the 35450–35650 cm^{-1} (282.09–280.50 nm) region.^{2–6} This indicates that the difference in the UV transition energy is less than 1% between these different conformers. The UV bands of different conformers cannot be distinguished from each other in solution, but a combination of several gas-phase techniques, such as supersonic jets and ion cooling in cryogenic ion traps, makes it possible to resolve these closely neighboring bands.^{7–9} Well-resolved UV spectral features in turn enable conformer-specific spectroscopies such as UV-UV hole-burning and IR-UV double-resonance, even for large systems.¹

Electronic spectroscopy in the gas phase under cold conditions has been applied to a number of molecular and non-covalently bound systems because of its high conformational resolving power.¹ However, one of its drawbacks is that it needs suitable chromophores; one cannot apply the above-mentioned techniques to systems that do not have strong absorption in the UV–visible region. One possibility to overcome this difficulty is to attach a UV–visible chromophore to the systems that we want to examine. One candidate for such a chromophore is a lanthanide ion (Ln^{3+}). Lanthanide ions show sharp f-f absorption and emission in the visible-to-UV region, even in solution.^{10, 11, 12} Hence, it is expected that the electronic transitions of lanthanide ions can be used to distinguish different conformers of molecules that do not have strong absorption in the UV–visible region, if the interaction between the ion and the molecule does not substantially affect the conformation.

For this purpose, we must first develop a new technique or find favorable conditions under which to produce lanthanide ion complexes in the gas phase. In addition, we need spectroscopic information of lanthanide ions themselves in the gas phase for comparison of electronic spectra. In our previous study, we tried to produce Ln^{3+} ions in the gas phase by using an electrospray ionization (ESI) source, but it was not possible to produce bare Ln^{3+} ions or Ln^{3+} complexes because of the effective charge transfer from Ln^{3+} to solvent molecules in the ESI process.¹³ Nevertheless, we found that an ESI source can produce some interesting lanthanide-containing ions, which may be useful for future electronic spectroscopy of large systems.

In this study, as a first step towards the application of lanthanide ions to the UV spectroscopy of large, cryogenically cooled molecules in the gas phase, we produce lanthanide-containing ions by electrospraying solutions of $\text{EuCl}_3 \cdot 6\text{H}_2\text{O}$ and $\text{TbCl}_3 \cdot 6\text{H}_2\text{O}$. This approach does not provide Eu^{3+} , Tb^{3+} , or their complexes, but we detect EuOH^+ , EuCl^+ , and TbO^+ ions in mass spectra. We measure gas-phase UV spectra of these ions by UV photodissociation (UVPD) spectroscopy in a cold, 22-pole ion trap. The UVPD spectra are analyzed with the aid of density functional theory (DFT) calculations that include relativistic effects. This work suggests the possibility of using lanthanide ions as “conformation reporters” for the gas-phase spectroscopy for large molecules.

2. Experimental and computational methods

The experiment is performed with a tandem mass spectrometer equipped with a nanoelectrospray ion source,⁷⁻⁹ through which we inject a solution of $\text{EuCl}_3 \cdot 6\text{H}_2\text{O}$ or $\text{TbCl}_3 \cdot 6\text{H}_2\text{O}$ ($\sim 200 \mu\text{M}$ each) in methanol/water ($\sim 98:2$ volume ratio). The parent ions of interest are selected by a quadrupole mass filter and introduced into a 22-pole RF ion trap, which is cooled by a closed-cycle He refrigerator to 6 K. The trapped ions are

cooled internally and translationally to ~ 10 K through collisions with cold He buffer gas,^{7, 8, 14, 15} which is pulsed into the trap. The trapped ions are then irradiated with a tunable UV laser pulse, which causes some fraction of them to dissociate. The resulting charged photofragments, as well as the remaining parent ions, are released from the trap, analyzed by a second quadrupole mass filter, and detected with a channeltron electron multiplier. The UVPD spectra of parent ions are obtained by plotting the yield of a particular photofragment ion as a function of the wavenumber of the UV laser. The UV light comes from the frequency-doubled output of a dye laser, which is pumped with the third or second harmonic of a nanosecond Nd:YAG laser with a repetition rate of 20 Hz. The UV laser power is ~ 1.5 mJ/pulse, and the UV laser is focused in the ion trap by using a quartz lens with a focal length of 500 mm. We also measure infrared spectra using IR-UV double-resonance spectroscopy. In these experiments, the output pulse of an IR optical parametric oscillator (OPO) precedes the UV pulse by ~ 100 ns and counter-propagates collinearly with it through the ion trap. Absorption of the IR light by the ions induces the depopulation of the vibrational and electronic ground state, resulting in the reduction of the net UV absorption.¹⁶ The wavenumber of the UV laser is then fixed to a vibronic transition for monitoring the IR-induced depletion of the UVPD yield, and the wavenumber of the OPO is scanned in the OH stretching region ($3500\text{--}3800\text{ cm}^{-1}$) while monitoring the number of fragment ions. IR-UV depletion spectra are obtained by plotting the yield of a particular photofragment as a function of the OPO wavenumber.

We also perform quantum chemical calculations for EuOH^+ , EuCl^+ , and TbO^+ ions using all-electron relativistic DFT calculations.^{17, 18} All DFT calculations are performed using the program ORCA ver. 3.0.0 developed by Neese.¹⁹ The scalar-relativistic zero-order regular approximation (ZORA) Hamiltonian, which

includes the atomic model potential and the perturbative treatment of the Breit-Pauli spin-orbit coupling term, is employed to consider the relativistic effect.²⁰ Segmented all-electron relativistic contracted (SARC2) Gaussian-type basis sets are assigned to Eu and Tb as QZV (61¹⁷/51¹¹/41⁸/41³) with three g-type polarization functions.^{21,22} For O, H, and Cl atoms, SVP and TZVP basis sets recontracted for ZORA Hamiltonian are used for geometry optimization and single-point calculation, respectively. We employ TPSSh functionals for both of optimization and single-point calculation, because they were used to examine the complex structure of lanthanide (III) ions.^{23,24}

3. Results and discussion

Figure 1 shows the mass spectra measured with (a) $\text{EuCl}_3 \cdot 6\text{H}_2\text{O}$ and (b) $\text{TbCl}_3 \cdot 6\text{H}_2\text{O}$ solutions. Doubly or triply charged ions such as Eu^{3+} , Eu^{2+} , Tb^{3+} , Tb^{2+} , or their complexes are not detected in our experiment. Since europium has two isotopes, ^{151}Eu and ^{153}Eu , in an abundance ratio of 48% and 52%, respectively, it is easy to identify ions containing a Eu atom in the mass spectra. In the mass spectrum of the Eu solution (Fig. 1a), Eu^+ , EuOH^+ , and EuCl^+ generate strong signals. In addition, strong peaks are found at $m/z = 209.9$ and 211.9 . These ions may correspond to $\text{EuC}_2\text{O}_2\text{H}_3^+$ or $\text{EuC}_3\text{O}_1\text{H}_7^+$, although the chemical composition or structure is not clear at the moment. Other strong peaks above $m/z = 200$ are attributed to solvated clusters of the ions at $m/z = 209.9$ and 211.9 .

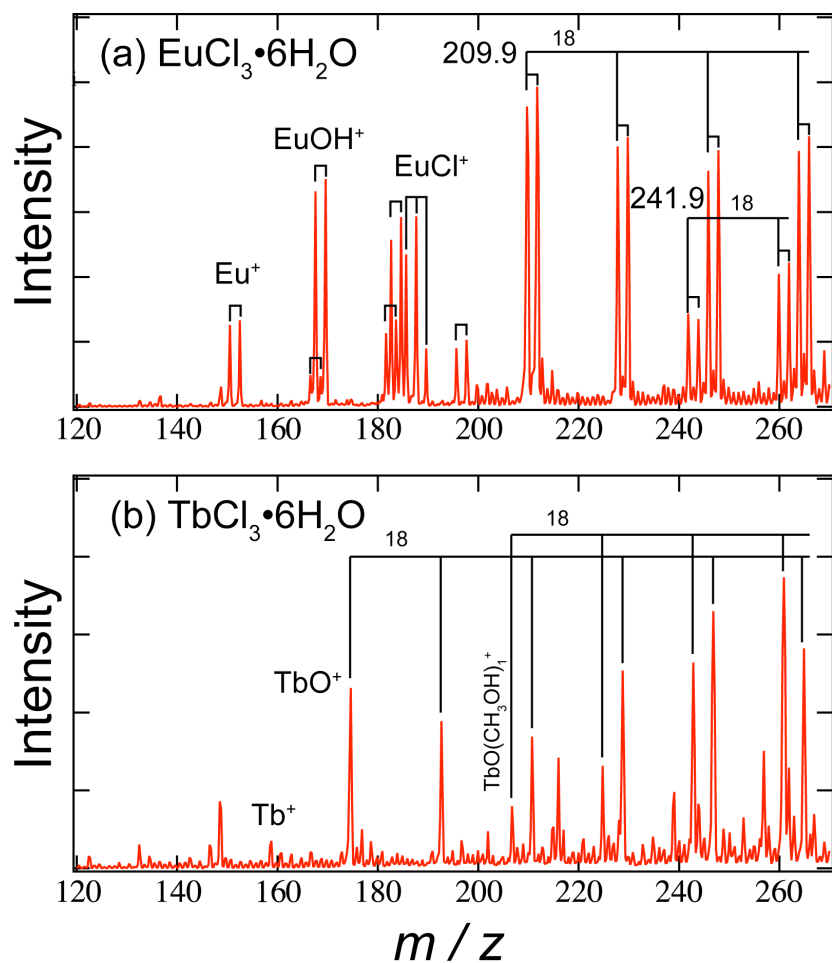


Figure 1. ESI mass spectra of (a) $\text{EuCl}_3 \cdot 6\text{H}_2\text{O}$ and (b) $\text{TbCl}_3 \cdot 6\text{H}_2\text{O}$.

The mass spectrum of the Tb system (Fig. 1b) is simpler than that of Eu, because Tb has only a single stable isotope, ^{159}Tb . In the mass spectrum of the Tb system, the Tb^+ ion produces only a small feature. Moreover, in contrast to the case of Eu, TbOH^+ or TbCl^+ is not found, while the peak corresponding to TbO^+ is quite strong in the mass spectrum. The signals above $m/z = 180$ can be ascribed to solvated clusters of TbO^+ . Among these ions in the mass spectra, the EuOH^+ , EuCl^+ , and TbO^+ ions show sharp UV bands in UVPD experiments.

Figure 2 displays UVPD spectra of the EuOH^+ , EuCl^+ , and TbO^+ ions. For the Eu ions, we mass-select the $^{151}\text{EuOH}^+$ and $^{151}\text{Eu}^{35}\text{Cl}^+$ ions and measure their UVPD spectra. The fragment ion monitored for the UVPD spectra is Eu^+ for EuOH^+ and EuCl^+ and Tb^+ for TbO^+ . All spectra show highly congested features with a number of sharp, well-resolved bands. The spectra are not simple like those of alkali metal ion complexes with aromatic molecules – they show no regular pattern of vibrational progressions.^{8,9,25} It is thus difficult to assign the UV bands definitely at the present stage. The UVPD data of the EuOH^+ , EuCl^+ , and TbO^+ ions are given in the Supporting Information as an Excel file.

In spite of the difficulty of the spectral assignment, well-resolved spectral features enable us to perform IR-UV double-resonance spectroscopy for a specific vibronic band. Figure 3 shows an IR-UV double-resonance spectrum of the EuOH^+ ion in the OH stretching region. This spectrum is measured at a probe position of 31596 cm^{-1} , shown with an arrow in Fig. 2a. A sharp depletion is observed at 3732 cm^{-1} , and this is assigned to the OH stretching vibration. This OH stretch frequency is close to that of transition metal hydroxide molecules, $\text{M}(\text{OH})_2$ ($\text{M} = \text{Mn}$ and Fe).²⁶

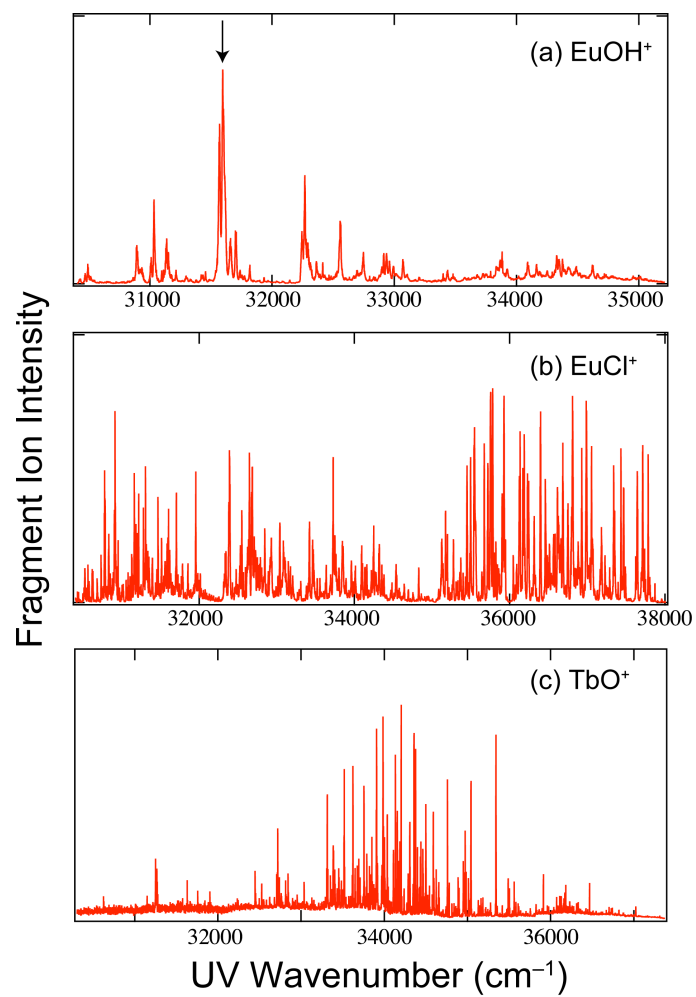


Figure 2. UVPD spectra of (a) EuOH^+ , (b) EuCl^+ , and (c) TbO^+ . The arrow in Fig. 2a shows the probe position for IR-UV double-resonance spectroscopy of EuOH^+ (see Fig. 3).

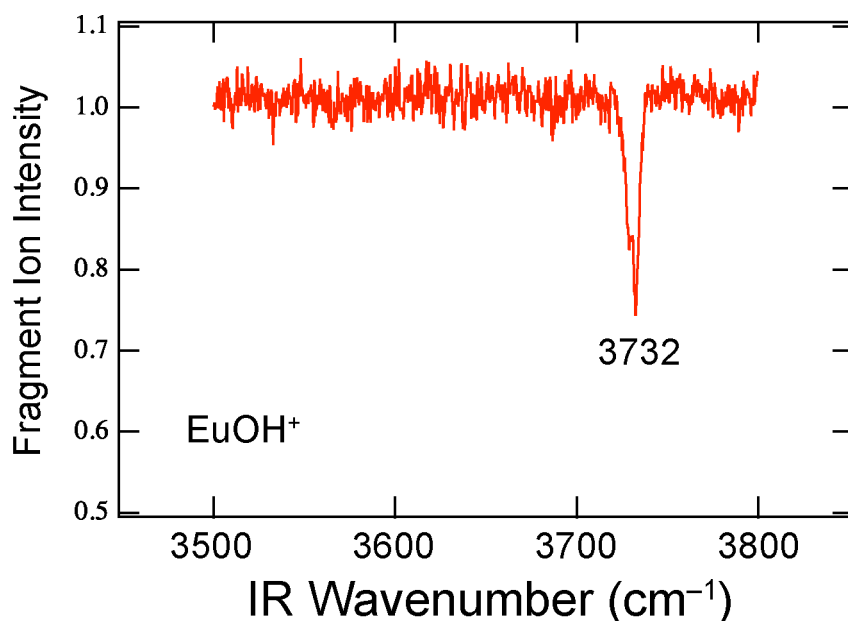


Figure 3. The IR-UV spectrum of the EuOH^+ ion in the OH stretching region.

We perform DFT calculations to examine the nature of the UV transitions. We first check the relative stability of different spin states. Table 1 shows the total energy of possible spin states for the EuOH^+ , EuCl^+ , and TbO^+ ions calculated at the TPSSh/TZVP level. For all the ions, the states of highest spin multiplicity (octet for EuOH^+ and EuCl^+ , and septet for TbO^+) are significantly more stable than other states of lower spin multiplicity. Hence, the EuOH^+ , EuCl^+ , and TbO^+ ions in our gas-phase experiments occupy these states of highest spin multiplicity.

Table 1. Total energy of each spin state for EuOH^+ , EuCl^+ , and TbO^+ calculated at the TPSSh/TZVP level of theory.

ions	spin state	E_{tot} hartree	ΔE_{tot} kJ/mol
EuOH^+	octet	-11155.859	0
	sextet	-11155.765	248
	quartet	-11155.706	402
	doublet	-11155.695	430
EuCl^+	octet	-11542.416	0
	sextet	-11542.318	257
	quartet	-11542.261	406
	doublet	-11542.252	430
TbO^+	septet	-12055.822	0
	quintet	-12055.747	197
	triplet	-12055.706	305
	singlet	-12055.694	337

We then calculate the electronic transition energy and oscillator strength of these ions in the UV region. The calculated results are collected in Tables 2–4. The molecular orbitals (MOs) that contribute the most to each of the electronic transitions in Tables 2–4 are shown in the Supporting Information. For the EuOH^+ ion, three strong UV transitions (transitions 1–3 in Table 2) exist in this region, and they correspond to electron promotion from the 4f to the (5d, 6p) orbitals of Eu ($\text{Eu}(4f) \rightarrow \text{Eu}(5d, 6p)$). The TD-DFT calculation of the EuOH^+ ion shows two other transitions (transitions 4 and 5) on the higher frequency side. These are due to electron transfer from O(2p) to Eu(6s), $\text{O}(2p) \rightarrow \text{Eu}(6s)$, but the oscillator strengths are one order of magnitude smaller than that of the above Eu transitions. From these TD-DFT results, we can assign the UV transitions of the EuOH^+ ion (Fig. 2a) to the $\text{Eu}(4f) \rightarrow \text{Eu}(5d, 6p)$ transitions. A similar trend can be seen for the EuCl^+ ion. Table 3 shows the TD-DFT results of the EuCl^+ ion. The strongest transition of EuCl^+ (transition 5) is due to the $\text{Eu}(4f) \rightarrow \text{Eu}(5d, 6p)$ electron promotion. Transitions 1 and 2 of the EuCl^+ ion are also ascribed to $\text{Eu}(4f) \rightarrow \text{Eu}(5d, 6p)$. The electronic transitions from Cl to Eu, $\text{Cl}(3p) \rightarrow \text{Eu}(6s)$, are one order of magnitude weaker than the $\text{Eu}(4f) \rightarrow \text{Eu}(5d, 6p)$ transitions. Hence, the UV absorption in the UVPD spectrum of the EuCl^+ ion can be assigned mainly to the $\text{Eu}(4f) \rightarrow \text{Eu}(5d, 6p)$ transition.

Table 2. Excitation energy, oscillator strength, and transition characters of EuOH^+ calculated at the TPSSh/TZVP level of theory.

Transition No.	Energy cm^{-1}	Oscillator strength	Composition	%	Assignment
1	31944	0.0247	$37\alpha \rightarrow 44\alpha$	39	$\text{Eu}(4f) \rightarrow \text{Eu}(5d,6p)$
			$34\alpha \rightarrow 42\alpha$	20	
			$35\alpha \rightarrow 43\alpha$	20	
2	31944	0.0247	$36\alpha \rightarrow 44\alpha$	31	$\text{Eu}(4f) \rightarrow \text{Eu}(5d,6p)$
			$34\alpha \rightarrow 43\alpha$	20	
			$35\alpha \rightarrow 42\alpha$	20	
3	32986	0.0585	$38\alpha \rightarrow 44\alpha$	37	$\text{Eu}(4f) \rightarrow \text{Eu}(5d,6p)$
			$37\alpha \rightarrow 43\alpha$	22	
			$36\alpha \rightarrow 42\alpha$	17	
4	37733	0.0034	$31\alpha \rightarrow 39\alpha$	99	$\text{O}(2p) \rightarrow \text{Eu}(6s)$
5	37767	0.0033	$30\alpha \rightarrow 39\alpha$	99	$\text{O}(2p) \rightarrow \text{Eu}(6s)$

Table 3. Excitation energy, oscillator strength, and transition characters of EuCl^+ calculated at the TPSSh/TZVP level of theory.

Transition No.	Energy cm^{-1}	Oscillator strength	Composition	%	Assignment
1	33469	0.0214	$41\alpha \rightarrow 48\alpha$	52	$\text{Eu}(4f) \rightarrow \text{Eu}(5d,6p)$
			$38\alpha \rightarrow 46\alpha$	10	
			$39\alpha \rightarrow 47\alpha$	10	
2	33469	0.0214	$40\alpha \rightarrow 48\alpha$	52	$\text{Eu}(4f) \rightarrow \text{Eu}(5d,6p)$
			$38\alpha \rightarrow 47\alpha$	10	
			$39\alpha \rightarrow 46\alpha$	10	
3	34343	0.0098	$35\alpha \rightarrow 43\alpha$	91	$\text{Cl}(3p) \rightarrow \text{Eu}(6s)$
4	34343	0.0098	$34\alpha \rightarrow 43\alpha$	91	$\text{Cl}(3p) \rightarrow \text{Eu}(6s)$
5	34352	0.0570	$42\alpha \rightarrow 48\alpha$	57	$\text{Eu}(4f) \rightarrow \text{Eu}(5d,6p)$
			$40\alpha \rightarrow 47\alpha$	15	
			$41\alpha \rightarrow 46\alpha$	15	
6	37537	0.0075	$35\beta \rightarrow 36\beta$	95	$\text{Cl}(3p) \rightarrow \text{Eu}(6s)$
7	37537	0.0075	$34\beta \rightarrow 36\beta$	95	$\text{Cl}(3p) \rightarrow \text{Eu}(6s)$
8	38315	0.0061	$33\alpha \rightarrow 43\alpha$	94	$\text{Cl}(3p) \rightarrow \text{Eu}(6s)$

Table 4. Excitation energy, oscillator strength, and transition characters of TbO^+ calculated at the TPSSh/TZVP level of theory.

Transition No.	Energy cm^{-1}	Oscillator strength	Composition	%	Assignment
1	30513	0.0020	$32\beta \rightarrow 40\beta$	49	$\text{Tb}(4f) \rightarrow \text{Tb}(5d)$
			$32\beta \rightarrow 39\beta$	36	
2	30573	0.0020	$32\beta \rightarrow 39\beta$	49	$\text{Tb}(4f) \rightarrow \text{Tb}(5d)$
			$32\beta \rightarrow 40\beta$	36	
3	31022	0.0034	$38\alpha \rightarrow 39\alpha$	97	$\text{O}(2p) \rightarrow \text{Tb}(6s)$
4	31677	0.0019	$29\beta \rightarrow 33\beta$	72	$\text{O}(2p) \rightarrow \text{Tb}(4f)$
			$30\beta \rightarrow 33\beta$	11	
5	31683	0.0019	$30\beta \rightarrow 33\beta$	72	$\text{O}(2p) \rightarrow \text{Tb}(4f)$
			$29\beta \rightarrow 33\beta$	11	
6	34567	0.0008	$37\alpha \rightarrow 39\alpha$	92	$\text{O}(2p) \rightarrow \text{Tb}(6s)$
7	34576	0.0008	$36\alpha \rightarrow 39\alpha$	92	$\text{O}(2p) \rightarrow \text{Tb}(6s)$
8	35122	0.0021	$29\beta \rightarrow 37\beta$	30	$\text{O}(2p) \rightarrow \text{Tb}(4f)$
			$30\beta \rightarrow 36\beta$	22	
			$29\beta \rightarrow 36\beta$	20	
			$30\beta \rightarrow 37\beta$	20	
9	35177	0.0022	$30\beta \rightarrow 37\beta$	30	$\text{O}(2p) \rightarrow \text{Tb}(4f)$
			$30\beta \rightarrow 36\beta$	22	
			$29\beta \rightarrow 36\beta$	22	
			$29\beta \rightarrow 37\beta$	17	
10	35342	0.0054	$31\beta \rightarrow 38\beta$	98	$\text{O}(2p) \rightarrow \text{Tb}(6s)$

In contrast, the TbO^+ ion shows a qualitatively different electronic spectrum. As seen in Table 4, the TbO^+ ion has 10 electronic transitions with comparable intensity. Among these 10 transitions, only two (transitions 1 and 2 in Table 4) has a localized character, $\text{Tb}(4f) \rightarrow \text{Tb}(5d)$, but the other 8 transitions have charge-transfer natures between O to Tb, $\text{O}(2p) \rightarrow \text{Tb}(4f, 6s)$. Therefore, the UV transition in the UVPD spectrum of the TbO^+ ion can be ascribed mainly to the charge-transfer transitions between O and Tb.

Table 5 shows the binding energy (E_{bind}) for the EuOH^+ , EuCl^+ , and TbO^+ ions calculated at the TPSSh/TZVP level of theory. The E_{bind} values in Table 5 are larger than 439 kJ/mol, which corresponds to $\sim 36900 \text{ cm}^{-1}$. Hence, the photodissociation of the EuOH^+ , EuCl^+ , and TbO^+ ions in the present UVPD experiment can occur via a two-photon absorption process.

Table 5. Binding energy (E_{bind}) of EuOH^+ , EuCl^+ , and TbO^+ calculated at the TPSSh/TZVP level of theory.

ion	$E_{\text{tot}}(\text{MX}^+)$ hartree	$E_{\text{tot}}(\text{M}^+)$ hartree	$E_{\text{tot}}(\text{X})$ hartree	E_{bind}^a kJ/mol
EuOH^+	-11154.728	-11078.695	-75.850	479
EuCl^+	-11541.286	-11078.695	-462.423	439
TbO^+	-12056.210	-11980.780	-75.185	640

$$^a E_{\text{bind}} = [E_{\text{tot}}(\text{M}^+) + E_{\text{tot}}(\text{X})] - E_{\text{tot}}(\text{MX}^+)$$

4. Summary

In summary, we apply UV and IR spectroscopy in the gas phase to the lanthanide-containing ions, EuOH^+ , EuCl^+ , and TbO^+ , which are cryogenically cooled in a cold, 22-pole ion trap. The UVPD spectra of these ions show a number of sharp, well-resolved vibronic bands. We also perform IR-UV double-resonance spectroscopy for the EuOH^+ ion, and the OH stretching vibration is observed at 3732 cm^{-1} . The DFT calculations suggest that these ions take the states of highest spin multiplicity (octet for EuOH^+ and EuCl^+ , and septet for TbO^+). For the EuOH^+ and EuCl^+ ions, the UV absorption can be attributed to the electron promotion from $\text{Eu}(4f)$ to $\text{Eu}(5d, 6p)$. In contrast, the TbO^+ ion has strong charge-transfer transitions assignable to $\text{O}(2p) \rightarrow \text{Tb}(4f, 6s)$ in addition to $\text{Tb}(4f) \rightarrow \text{Tb}(5d)$. Now that we can perform UV-UV hole-burning spectroscopy of cryogenically cooled ions, it would be possible to discriminate transitions that share the same, initial rotational levels, which will make the assignment of the congested spectra much easier.²⁷ The analysis of these complicated spectra by experimental and theoretical investigation is ongoing in our laboratory. The UVPD spectra of the EuOH^+ , EuCl^+ , and TbO^+ ions show very sharp bands, which

suggests that it will be possible to use lanthanide-containing ions as “conformation reporters” for large molecules that do not have strong absorption in the UV–visible region. However, the EuOH^+ , EuCl^+ , and TbO^+ ions seem not to be so suitable for UV spectroscopy of large systems because of their very congested UV spectra. As reported in previous papers, Ln^{3+} ions such as Eu^{3+} and Tb^{3+} show sharp bands but much simpler spectral features in solution than those of EuOH^+ , EuCl^+ , and TbO^+ .^{10, 11} In order to use Ln^{3+} ions as a chromophore for gas-phase spectroscopy, we have to develop a way to avoid charge transfer from lanthanide ions to solvent molecules and to attach them to systems of interest in ESI sources.

Supporting Information Available: The data of the UVPD spectra for the EuOH^+ , EuCl^+ , and TbO^+ ions as an Excel file (UVPD.xlsx). The MOs that contribute to the most to the electronic transitions of the EuOH^+ , EuCl^+ , and TbO^+ ions.

Acknowledgment

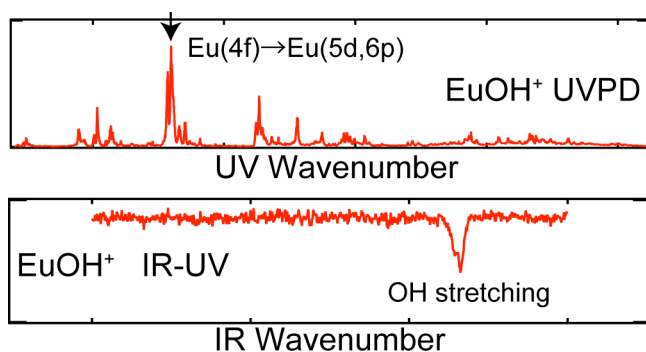
This work was partly supported by JSPS KAKENHI Grant Number 16H04098 and by the Swiss National Science Foundation under grant number 200020_152804.

References

- (1) Rizzo, T. R.; Boyarkin, O. V. Cryogenic Methods for the Spectroscopy of Large, Biomolecular Ions. *Gas-Phase IR Spectroscopy and Structure of Biological Molecules* **2015**, 364, 43-97.
- (2) Martinez, S. J.; Alfano, J. C.; Levy, D. H. The electronic spectroscopy of the amino acids tyrosine and phenylalanine in a supersonic jet. *J. Mol. Spectrosc.* **1992**, 156, 421-430.
- (3) Grace, L. I.; Cohen, R.; Dunn, T. M.; Lubman, D. M.; de Vries, M. S. The R2PI Spectroscopy of Tyrosine: A Vibronic Analysis. *J. Mol. Spectrosc.* **2002**, 215, 204-219.
- (4) Inokuchi, Y.; Kobayashi, Y.; Ito, T.; Ebata, T. Conformation of L-Tyrosine Studied by Fluorescence-Detected UV-UV and IR-UV Double-Resonance Spectroscopy. *J. Phys. Chem. A* **2007**, 111, 3209-3215.
- (5) Shimozone, Y.; Yamada, K.; Ishiuchi, S.-i.; Tsukiyama, K.; Fujii, M. Revised Conformational Assignments and Conformational Evolution of Tyrosine by Laser Desorption Supersonic Jet Laser Spectroscopy. *Phys. Chem. Chem. Phys.* **2013**, 15, 5163-5175.
- (6) Abo-Riziq, A.; Grace, L.; Crews, B.; Callahan, M. P.; van Mourik, T.; Vries, M. S. d. Conformational Structure of Tyrosine, Tyrosyl-Glycine, and Tyrosyl-Glycyl-Glycine by Double Resonance Spectroscopy. *J. Phys. Chem. A* **2011**, 115, 6077-6087.
- (7) Svendsen, A.; Lorenz, U. J.; Boyarkin, O. V.; Rizzo, T. R. A New Tandem Mass Spectrometer for Photofragment Spectroscopy of Cold, Gas-Phase Molecular Ions. *Rev. Sci. Instrum.* **2010**, 81, 073107.
- (8) Inokuchi, Y.; Boyarkin, O. V.; Kusaka, R.; Haino, T.; Ebata, T.; Rizzo, T. R. UV and IR Spectroscopic Studies of Cold Alkali Metal Ion-Crown Ether Complexes in the Gas Phase. *J. Am. Chem. Soc.* **2011**, 133, 12256-12263.
- (9) Inokuchi, Y.; Ebata, T.; Rizzo, T. R.; Boyarkin, O. V. Microhydration Effects on the Encapsulation of Potassium Ion by Dibenzo-18-Crown-6. *J. Am. Chem. Soc.* **2014**, 136, 1815-1824.
- (10) Carnall, W. T.; Fields, P. R.; Rajnak, K. Electronic Energy Levels of Trivalent Lanthanide Aquo Ions 4. Eu^{3+} . *J. Chem. Phys.* **1968**, 49, 4450-4455.
- (11) Carnall, W. T.; Fields, P. R.; Rajnak, K. Electronic Energy Levels of Trivalent Lanthanide Aquo Ions 3. Tb^{3+} . *J. Chem. Phys.* **1968**, 49, 4447-4449.
- (12) Cotton, S., *Lanthanide and Actinide Chemistry*. John Wiley & Sons, Ltd.: United States of America, 2006.
- (13) Inokuchi, Y.; Ebata, T.; Rizzo, T. R. UV and IR Spectroscopy of Cold H_2O^+ -Benzo-Crown Ether Complexes. *J. Phys. Chem. A* **2015**, 119, 11113-11118.
- (14) Boyarkin, O. V.; Mercier, S. R.; Kamariotis, A.; Rizzo, T. R. Electronic Spectroscopy of Cold, Protonated Tryptophan and Tyrosine. *J. Am. Chem. Soc.* **2006**, 128, 2816-2817.
- (15) Rizzo, T. R.; Stearns, J. A.; Boyarkin, O. V. Spectroscopic Studies of Cold, Gas-Phase Biomolecular Ions. *Int. Rev. Phys. Chem.* **2009**, 28, 481-515.
- (16) Nagornova, N. S.; Rizzo, T. R.; Boyarkin, O. V. Exploring the Mechanism of IR-UV Double-Resonance for Quantitative Spectroscopy of Protonated Polypeptides and Proteins. *Angew. Chem. Int. Ed.* **2013**, 52, 6002-6005.
- (17) Kaneko, M.; Miyashita, S.; Nakashima, S. Bonding Study on the Chemical Separation of Am(III) from Eu(III) by S-, N-, and O-Donor Ligands by Means of All-Electron ZORA-DFT Calculation. *Inorg. Chem.* **2015**, 54, 7103-7109.

- (18) Kaneko, M.; Miyashita, S.; Nakashima, S. Benchmark Study of the Mossbauer Isomer Shifts of Eu and Np Complexes by Relativistic DFT Calculations for Understanding the Bonding Nature of f-block Compounds. *Dalton Trans.* **2015**, *44*, 8080-8088.
- (19) Neese, F. The ORCA Program System. *Wiley Interdisciplinary Reviews-Computational Molecular Science* **2012**, *2*, 73-78.
- (20) van Wullen, C. Molecular Density Functional Calculations in the Regular Relativistic Approximation: Method, Application to Coinage Metal Diatomics, Hydrides, Fluorides and Chlorides, and Comparison with First-Order Relativistic Calculations. *J. Chem. Phys.* **1998**, *109*, 392-399.
- (21) Pantazis, D. A.; Neese, F. All-Electron Scalar Relativistic Basis Sets for the Lanthanides. *J. Chem. Theory Comput.* **2009**, *5*, 2229-2238.
- (22) Aravena, D.; Neese, F.; Pantazis, D. A. Improved Segmented All-Electron Relativistically Contracted Basis Sets for the Lanthanides. *J. Chem. Theory Comput.* **2016**, *12*, 1148-1156.
- (23) Fang, M.; Bates, J. E.; Lorenz, S. E.; Lee, D. S.; Rego, D. B.; Ziller, J. W.; Furche, F.; Evans, W. J. (N₂)³⁻ Radical Chemistry via Trivalent Lanthanide Salt/Alkali Metal Reduction of Dinitrogen: New Syntheses and Examples of (N₂)²⁻ and (N₂)³⁻ Complexes and Density Functional Theory Comparisons of Closed Shell Sc³⁺, Y³⁺, and Lu³⁺ versus 4f⁹ Dy³⁺. *Inorg. Chem.* **2011**, *50*, 1459-1469.
- (24) Martins, A. F.; Eliseeva, S. V.; Carvalho, H. F.; Teixeira, J. M. C.; Paula, C. T. B.; Hermann, P.; Platas-Iglesias, C.; Petoud, S.; Tóth, É.; Geraldes, C. F. G. C. A Bis(pyridine *N*-oxide) Analogue of DOTA: Relaxometric Properties of the Gd^{III} Complex and Efficient Sensitization of Visible and NIR-Emitting Lanthanide(III) Cations Including Pr^{III} and Ho^{III}. *Chem. Eur. J.* **2014**, *20*, 14834-14845.
- (25) Inokuchi, Y.; Boyarkin, O. V.; Kusaka, R.; Haino, T.; Ebata, T.; Rizzo, T. R. Ion Selectivity of Crown Ethers Investigated by UV and IR Spectroscopy in a Cold Ion Trap. *J. Phys. Chem. A* **2012**, *116*, 4057-4068.
- (26) Wang, X.; Andrews, L. Infrared Spectra of M(OH)_{1,2,3} (M = Mn, Fe, Co, Ni) Molecules in Solid Argon and the Character of First Row Transition Metal Hydroxide Bonding. *J. Phys. Chem. A* **2006**, *110*, 10035-10045.
- (27) Inokuchi, Y.; Nakatsuma, M.; Kida, M.; Ebata, T. Conformation of Alkali Metal Ion–Benzo-12-Crown-4 Complexes Investigated by UV Photodissociation and UV–UV Hole-Burning Spectroscopy. *J. Phys. Chem. A* **2016**.

Table of Contents Synopsis



Ultraviolet photodissociation spectra of EuOH^+ , EuCl^+ , and TbCl^+ , which are produced by an electrospray ionization source and cooled to ~ 10 K in a cold, 22-pole ion trap, show a number of sharp, well-resolved bands. These results suggest the potentiality of lanthanide ions as “conformation reporters” of large molecules in the gas-phase spectroscopy under cold conditions.